ACS Partner Journal

ACCOUNTS
—of materials research—

pubs.acs.org/amrcda

Article

Single-Crystalline Hydrogen-Bonded Crosslinked Organic Frameworks and Their Dynamic Guest Sorption

Jayanta Samanta,[†] Yunjia Zhang,[†] Mingshi Zhang, Albert D. Chen, and Chenfeng Ke*

Cite This: https://doi.org/10.1021/accountsmr.2c00173

Read Online

ACCESS | Metrics & More | Article Recommendations

Downloaded via DARTMOUTH COLG on November 9, 2022 at 15:22:01 (UTC).
See https://pubs.acs.org/sharingguidelines for options on how to legitimately share published articles.

CONSPECTUS: Porous organic framework materials constructed by periodically aligned molecular entities offer chemically tailored microenvironments to absorb molecules and ions for various applications. Fundamentally understanding the microenvironments of these porous organic materials—from pore size, shape, and dynamics to potential substrate binding sites—is critical for the rational design of porous organic materials. The solid-state structures of these porous organic materials, such as covalent organic frameworks (COFs), can provide unambiguous atomic-level structural details. However, it remains challenging to synthesize these materials as single crystals that can be fully characterized by single-crystal X-ray diffraction (SCXRD) or rotational electron diffraction (RED) analysis. In addition, the balance of single crystallinity, permanent porosity, and good chemical stability requires delicate control of the assembly of the molecular building blocks and covalent crosslinking during synthesis. In this Account, we discuss the development of hydrogen-bonded crosslinked organic frameworks (H_COFs) possessing balanced single crystallinity and high chemical stability. H_COFs are obtained through covalently crosslinking molecular crystals that are preorganized via hydrogen bonding. Due to the dual hydrogen-bonded network and covalent crosslinking, H_COFs can deform upon guest adsorption by breaking the hydrogen bonds and subsequently restore their original form through the desorption of guests by re-establishing the hydrogen-bonded networks. Thus, H_COFs can dynamically adjust their pore sizes according to the framework−substrate interactions. In the discussion, we link H_COFs with COFs and single-crystalline 2D polymers by comparing their synthetic approaches to accessing high crystallinity. The method to synthesize H_COFs allows for the employment of various flexible building blocks and linking motifs that are largely avoided in the current design regimes of COFs and 2D polymers. We also draw the connections between H_COFs and hydrogen-bonded organic frameworks (HOFs) by highlighting their shared design principles for constructing hydrogen-bonding networks with large voids. Compared to their hydrogen-bonded precursor crystals, reinforcing the hydrogen-bonded networks with covalent linkages endows H_COFs with enhanced chemical and structural stability. In addition, we emphasize that the structure elucidation of H_COFs often requires combined SCXRD analysis and experimental evidence, with the methods and challenges thoroughly discussed. The details are presented in the following sequence: (1) synthesizing single-crystalline COFs by matching the polycondensation rate to the nucleation rate and their subsequent analyses by SCXRD/RED; (2) obtaining single-crystalline polymers and networks through topochemical reactions; (3) constructing HOFs with designed voids using highly directional hydrogen bonding building blocks; and (4) developing H_COFs via monomer crystal engineering followed by single-crystal to single-crystal (SCSC) synthesis and studying their unique dynamic guest sorption behaviors. We hope this Account will inspire researchers to expand the synthetic methods for advancing H_COFs with detailed solid-state structures, as well as designing porous organic framework materials with dynamic sorption capabilities to enhance their performance for applications in molecular storage, separation, catalysis, etc.

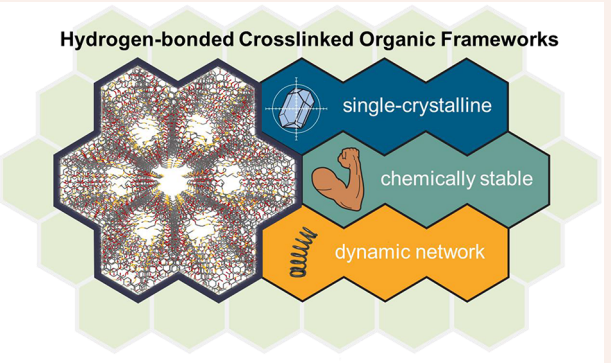

1. INTRODUCTION

Porous materials[1] that possess periodic, nanoscale voids have been investigated for decades for their applications in water purification,[2] petroleum products processing,[3] and energy conversion.[4] Taking advantage of these nanoscale voids, porous materials can selectively adsorb target molecular or ionic species and separate them from bulk or catalytically convert them to products of interest.[5] Zeolitic materials that carry out these processes have been produced on the scale of

Received: August 25, 2022
Revised: October 5, 2022

ACS Publications

© XXXX Accounts of Materials Research. Co-published by ShanghaiTech University and American Chemical Society. All rights reserved.

millions of tons for petrochemical separation and catalysis.[3] Since then, the family of porous materials has expanded to include metal−organic frameworks (MOFs),[6] covalent organic frameworks (COFs),[7] hydrogen-bonded organic frameworks (HOFs),[8] and recently, hydrogen-bonded crosslinked organic frameworks (H_COFs).[9] These organic frameworks represent a scientific advancement over zeolites by introducing modularity into the synthetic building blocks, providing the ability to design and tune the materials for targeted substrate sorption.[6]

Among these frameworks, COFs, HOFs, and H_COFs are composed purely of light elements. Due to their periodic organic struts, they offer exciting skeleton design and modification capabilities. An atomic-level understanding of the organic framework architecture and the detailed local chemical environment is vital to establishing the fundamental structure−property relationships. The resolved solid-state structures of the frameworks can reveal critical information such as the network topology, interpenetration and flexibility, local substrate binding sites, environments, and framework substrate interactions. Hence, obtaining porous organic framework single crystals suitable for single-crystal X-ray diffraction (SCXRD)[10,11] or rotation electron diffraction (RED)[12] is crucial. However, most COFs are polycrystalline powders not suitable for SCXRD analysis, making powder X-ray diffraction (PXRD) the most useful characterization tool for COFs. Typically, a COF's structure is verified by matching its simulated PXRD pattern with that obtained experimentally. Although the process has become widely accepted for structural elucidation of COFs, it has limitations in revealing stacking arrangements for two-dimensional COFs and interpenetration numbers for three-dimensional COFs.[10] It, therefore, remains challenging to comprehensively understand the structure−property relationships in a COF with atomic precision. In contrast to COFs, the construction of HOFs relies on weak interactions for the direct assembly of small-molecule building blocks, and HOFs are almost always obtained as single crystals. Since HOFs are connected via weak hydrogen bonds, they are considerably less stable than COFs. Hence, developing porous organic frameworks with high crystallinity and good chemical stability remains an overarching challenge associated with the development of porous organic framework materials.

To tackle this challenge, we introduced H_COFs as a new family of porous organic frameworks (Figure 1).[9,13−16] The design, synthesis, and characterization of H_COFs take inspiration from HOFs, COFs, and single-crystalline polymers.[17] H_COFs are synthesized in two steps: (1) self-assembly of monomers into porous hydrogen-bonded molecular crystals similar to HOFs; and (2) crosslinking of the preorganized porous molecular crystals using externally diffused flexible crosslinkers, resembling the synthesis of COFs and solid-state topochemical polymerizations. H_COFs not only possess high crystallinity for precise structure−property analysis and high chemical stability for chemical storage and separation, but they can also, very uniquely, be activated to an expanded state upon adsorbing guests with hydrogen bonding capabilities. Benefiting from their dual hydrogen-bonded and covalently crosslinked networks, the removal of guests allows H_COFs to (partially) return to their highly crystalline state. The guest-sorption-induced expansions and contractions of H_COFs are similar to traditional polymer networks (Figure 1), in which interpenetrated polymer chains recover their shape upon the removal of mechanical stress owing to the chains' tendency to maximize their randomness for entropy gain.

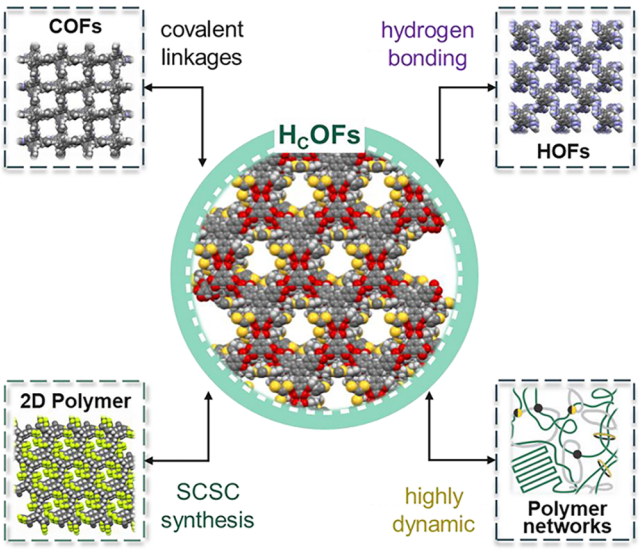

Figure 1. Connections between H_COFs and other organic materials, including COFs, HOFs, single-crystalline 2D polymers, and conventional polymer networks. The solid-state structures of COF-300,[10] HOF-1,[42] a single-crystalline 2D polymer,[34] and H_COF-101[15] are shown here.

Here, we first summarize different approaches to accessing single-crystalline COFs and polymers, including their synthetic strategies, single-crystal structural analysis, and the corresponding structure−property relationships. We emphasize the knowledge revealed by obtaining the solid-state structures, including three-dimensional stacking of building blocks, network topology, pore-size distributions, and network interpretation. Next, we survey methods to directionally assemble hydrogen-bonded networks using complementary hydrogen bonding motifs and different core building blocks. Collectively, these efforts inform the design, synthesis, and characterization of H_COFs. This Account provides step-by-step guidance in the synthesis and characterizations of single-crystalline H_COFs, as well as detailing the network topology in relation to their dynamic guest sorption properties. We hope the understanding of H_COFs can inspire future designs of HOFs and COFs and encourage more researchers to investigate H_COFs for a better understanding of the structure−property relationships in the development of porous organic materials.

2. ACCESSING SINGLE-CRYSTALLINE FRAMEWORKS AND POLYMERS

The rational synthesis of single-crystalline polymers, networks, and frameworks is not trivial. There have been two general approaches successfully demonstrated (1) utilization of highly reversible reactions and (2) solid-state topochemical synthesis through single-crystal to single-crystal (SCSC) transformations. In this section, we will discuss these two approaches and their connections to H_COF synthesis.

2.1. Single-Crystalline COFs

COFs (COF-1 and COF-5) were first synthesized by Yaghi et al.[18] through reversible boronic acid/ester condensation reactions (Figure 2a). These boronic acid/ester-based COF materials are polycrystalline, and their structures were

https://doi.org/10.1021/accountsmr.2c00173
Acc. Mater. Res. XXXX, XXX, XXX−XXX

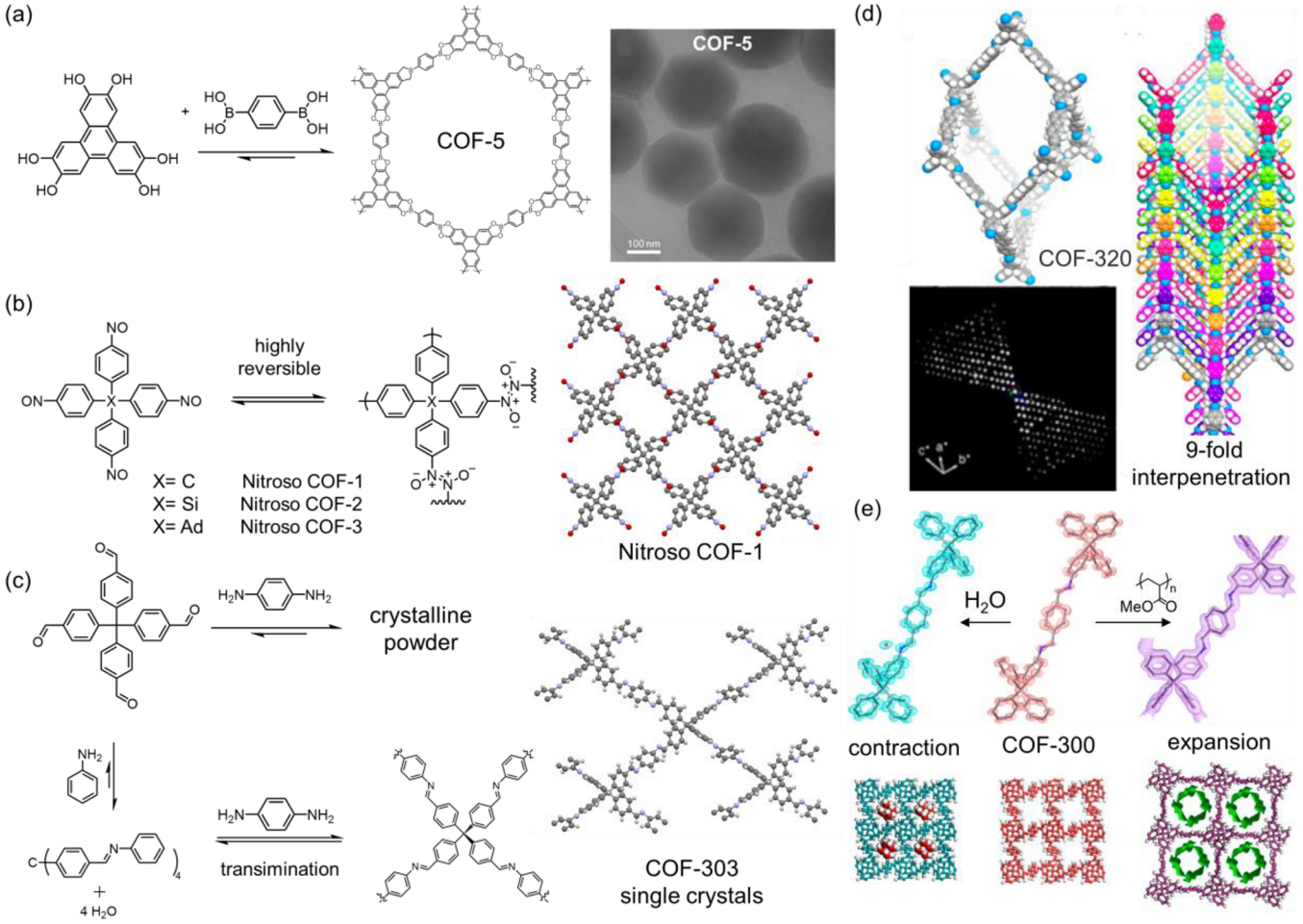

Figure 2. (a) Synthesis of COF-5 and a TEM image of COF-5 crystal. Reproduced with permission from ref 20. Copyright 2018 The American Association for the Advancement of Science. (b) Synthesis of Nitroso-COFs via a nitroso dimerization. Right: single-crystal structure of Nitroso-COF-1.[11] (c) Synthesis of single-crystalline imine-based COF-303 through transamination. Right: the single-crystal structure of COF-303.[10] (d) Solid-state structure of COF-320 with 9-fold interpenetration and their RED pattern. Reproduced with permission from ref 24. Copyright 2013 American Chemical Society. (e) Solid-state structures of active COF-300, COF-300·H_2O, and COF-300·poly(methyl methacrylate) (COF-300·PMMA). Reproduced with permission from ref 26. Copyright 2019 American Chemical Society.

elucidated through PXRD. Dichtel et al. attributed the formation of polycrystalline boronate ester-linked COFs to the irreversible stacking of the nanocrystallites.[19] Later, they reported single-crystalline boronic ester-based COFs through a seed growth method.[20] The crystallinity was confirmed through high-resolution TEM investigations, but the crystals were not big enough for SCXRD analysis.

Optimizing the reversibility of the reactions could improve the crystallinity of COFs. In 2013, Wuest et al. introduced the highly reversible nitroso dimerization reaction for COF synthesis.[11] The low bond energy of dinitroso enables room temperature covalent bond breakage and re-formation. Therefore, they successfully obtained a series of tetrakis(4-nitrosophenyl) methane/silane/adamantane-based single-crystalline COFs (Figure 2b), which are diamondoid networks with 4- or 6-fold interpenetration confirmed by SCXRD. Although these single crystals showed guest accessible void spaces of 35−39%, they did not exhibit permanent porosity, likely due to weak linkages.

The synthesis of COFs has expanded rapidly in the past decade, from examples such as the well-established imine (Figure 2c) and ketoenamine[21] condensations to other reversible reactions.[22] For imine COFs, Dichtel et al. suggested a model that includes nanocrystallite formation,[23] followed by polymerization to amorphous polymers, and then crystalline transformations for COFs. However, most COFs are polycrystalline powders, and their solid-state structures are largely proposed on the basis of their PXRD profiles. The key challenge preventing easy access to single-crystalline COFs is the mismatch of (de)polycondensation reaction rates ($k_{\text{bond-formation}}$ and $k_{\text{bond-rearrangement}}$) and the crystallization rates (nucleation and phase separation) during COF synthesis.[10]

In 2018, Wang and Yaghi et al. reported the first sets of single-crystalline imine COFs' solid-state structures (Figure 2c).[10] In this work, a large amount of aniline was added as a reaction rate modulator to match polycondensation and nucleation rates. As a result, large single crystals of imine-based COF-300, COF-303, LZU-79, and LZU-111 were obtained. It was also found by SCXRD analysis that the water molecules are arranged into infinite chains within the channel of COF-300. In the SCXRD structure, a 7-fold interpenetrated network of the COF-300 synthesized by the aniline modulator method was determined with atomic-level precision.

https://doi.org/10.1021/accountsmr.2c00173
Acc. Mater. Res. XXXX, XXX, XXX−XXX

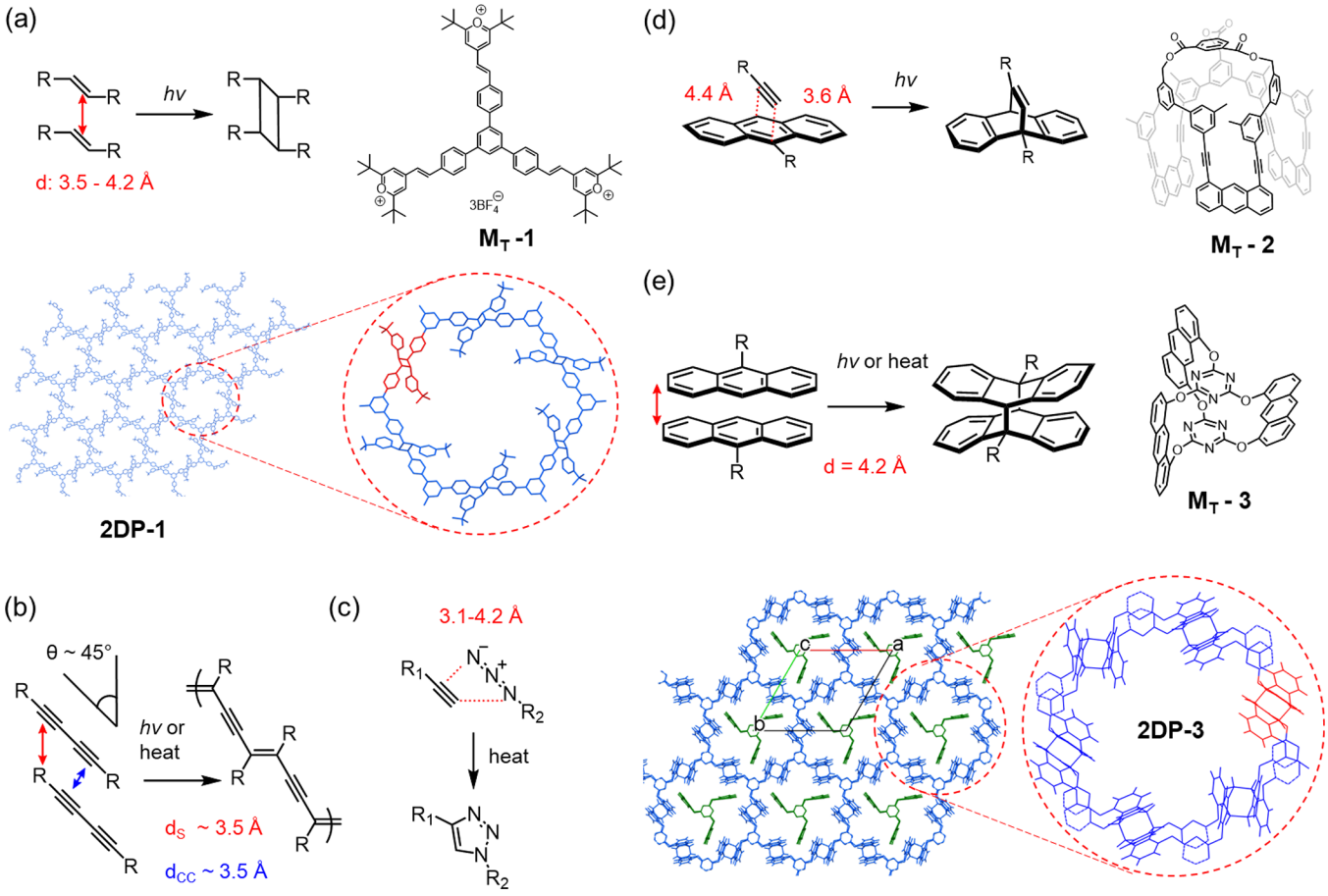

Figure 3. (a) Topochemical [2 + 2] cycloaddition and the synthesis of a single-crystalline 2D polymer sheet obtained from $\mathbf{M_T}$**-1**.[31] Solid-state (b) 1,3-diyne polymerization and (c) [3 + 2] azide−alkyne cycloaddition. (d) Topochemical [4 + 2] anthracene-alkyne cycloaddition and the monomer $\mathbf{M_T}$**-2** used for 2D polymer synthesis.[28] (e) [4 + 4] anthracene dimerization and the monomer $\mathbf{M_T}$**-3** used for 2D polymer synthesis.[33] Unreacted $\mathbf{M_T}$**-3** units removed for clarity. Packing distances between two diacetylenes d_S, distance between reactive carbons d_{CC}, and tilt angles θ are highlighted.

Aside from SCXRD, RED has recently been introduced for structure determination of single-crystalline framework materials.[12] Crystals viable for RED can be as small as 50 nm in diameter, while SCXRD analysis generally requires crystals larger than 5 μm. The structure of COF-320,[24] which was synthesized via imine condensation between dialdehyde and (tetraaminophenyl)methane, was characterized using RED as a 9-fold interpenetrated diamondoid network (Figure 2d). Using RED, Wang et al. discovered that single crystals of COF-300 with 5-fold interpenetration were transformed to a 7-fold interpenetrated diamond network upon aging.[25] Zhang et al. reported the framework dynamics of COF-300 upon guest adsorption. The structures of the activated phase of COF-300, its hydrated COF-300·H_2O form, and its expanded COF-300·PMMA form revealed atomic-level dynamics of the COFs (Figure 2e).[26] When the diffraction with RED is poor, it can partially refine the structure to construct the solid-state structures of COFs by computational modeling and refinement with the help of PXRD data.[27]

2.2. Topochemical Synthesis in the Solid State

Solid-state topochemical reactions provide another path to construct single-crystalline covalent polymers or networks.[17,28] In this approach, the organic building blocks are first organized by crystallization so that the reactive motifs are in close proximity for reaction under thermal or photochemical conditions. This transformation is often referred to as an SCSC transformation[17] if single crystallinity is retained. Early studies of [2 + 2] cyclobutane formation (Figure 3a) in crystals demonstrated the feasibility of topochemical reactions.[29] Today, besides [2 + 2] additions, other topochemical reactions including [3 + 2] azide−alkyne cycloaddition, [4 + 2] anthracene−alkyne cycloaddition, [4 + 4] anthracene−anthracene dimerization,[30] 1,4-dialkene addition, and diacetylene polymerization, have also been introduced into polymer or network synthesis (Figure 3).[28]

In a successful topochemical synthesis, reactive sites should be aligned in the suggested conformation and distance in the solid state (Figure 3). For example, in a [2 + 2] reaction, two olefins should be arranged in parallel within a distance of 3.5−4.2 Å.[29] 2D polymerization has been demonstrated using a pyrylium-based triolefinic monomer $\mathbf{M_T}$**-1** ($\mathbf{M_T}$ stands for monomer for topochemical synthesis),[31] in which $\mathbf{M_T}$**-1** were $\pi-\pi$ stacked and the olefin groups were parallel to each other with a distance of 3.9 Å. Other parameters such as tilt angle θ, carbon atom distance d_{CC}, and packing distance d_S should also be taken into consideration (Figure 3b,c).[28] Schlüter et al. prepared a crystal of $\mathbf{M_T}$**-2** packed so that the alkyne and anthracene distances (d_{CC} = 4.4 and 3.6 Å, Figure 3d) and their orientations were suitable for [4 + 2] cycloaddition.[32] After photoirradiation, the crystal was successfully polymerized as a 2D network. Later, they reported 2D polymerization of a

https://doi.org/10.1021/accountsmr.2c00173
Acc. Mater. Res. XXXX, XXX, XXX−XXX

triazene-based double-decker monomer $\mathbf{M_T}$-**3** (Figure 3e).[33] The anthracene blades were packed in a face-to-face (FTF, blue colored) manner and an edge-to-face (ETF, green colored) manner, and the crystal underwent FTF dimerization upon photoirradiation. King et al. reported a similar 2D polymer synthesis using a triptycene-based molecular crystal.[34] The internal stress generated during the SCSC process can shatter the crystal into smaller fragments. Moieties with rotatable bonds, such as C−C and C−O single bonds have been introduced to compensate for the internal stress.[35]

It is worth noting that the utilization of photobased SCSC transformations is particularly favored for single crystals containing large solvent-filled voids, e.g., in the case of H_COF synthesis, because photoreactions usually occur at ambient or low temperatures and therefore mitigate disruption to crystallinity during the SCSC transformation. Although no addition of external crosslinker is required in the homo-photodimerization-based SCSC transformation (Figure 3a,e), reaction-induced geometric changes in the molecular arrangement may be detrimental to the crystallinity of the final product. In comparison, the hetero-crosslinking strategy (discussed in Section 4) appears to be a more adaptive approach for H_COF development, provided that the crystalline molecular precursors form interconnected pores in the solid state large enough for crosslinkers to diffuse into.

3. MOLECULARLY ENGINEERING POROUS HYDROGEN-BONDED NETWORKS

HOFs are composed of monomers that are hydrogen-bonded to each other to form permanently porous frameworks[8,36−38] via a variety of hydrogen-bonding motifs that are attached to cores of different geometries (Figure 4). In HOFs, motifs with multivalent hydrogen bonding capabilities are generally employed to increase the hydrogen-bonding strength of the network. An early example of a hydrogen-bonded network reported in 1969 was synthesized by crystallizing trimesic acid (TA) with carboxylic acid dimer connections.[39] Later, Wuest et al. introduced **S1** (**S** stands for synthon, Figure 4a) as a complementary donor−acceptor (DA) hydrogen-bonding group to form a hydrogen-bonded network.[40] They also reported a diamondoid net formed by a **C6**/**S2** monomer (**C** stands for core, Figure 4) with 42% of void space filled by solvents.[41] A key milestone in developing HOF materials was achieved by Chen et al., when they demonstrated permanent porosity with HOF-1 (**C6**/**S2** monomer) in 2011.[42] The solvents were removed without disrupting the hydrogen-bonded network, and HOF-1 showed excellent separation of C_2H_4 from C_2H_2. We recently discovered that guests such as aniline and toluidine form cyclic tetramers[43] in the voids of HOF-1. The coadsorption of different guests enabled an alkylation reaction to take place inside HOF-1.

Compared to **S2**, which has a donor−acceptor−donor (DAD) hydrogen-bonding array, self-complementary carboxylic acids **S3** with a DA array (Figure 4a) are widely used to construct HOFs. Attaching phenyl carboxylic acid groups to **C1** and **C3** and **C4** affords a variety of HOFs with different network topologies and pore sizes.[38] In these HOFs, the carboxylic acid dimers are highly directional due to the $\mathbf{R}_2^2(8)$ hydrogen bonding connection. The topologies of these networks (without considering network interpenetration) are much more predictable compared to those formed by **S2**-based monomers. However, carboxylic acid-based HOFs are

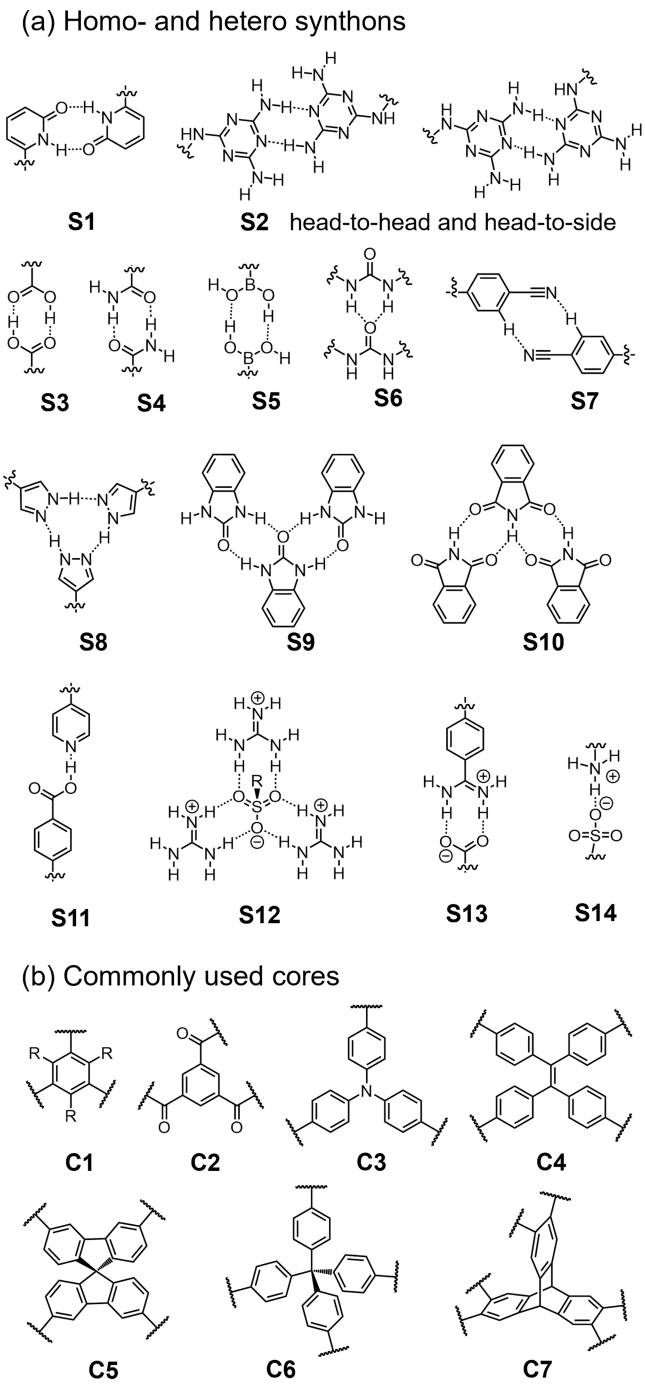

Figure 4. (a) Homo- and hetero-hydrogen bonding synthons and their corresponding hydrogen bonding patterns in HOFs' design. (b) Rigid core struts used for HOFs.

generally not stable under basic conditions. Other self-complementary hydrogen bonding synthons such as **S4**−**S6**, pyrazole **S8**,[44,45] maleimide **S9**,[46] and **S10** have also been used in the synthesis of HOFs.[36] Recently, a very weak C−N···H_{Ar} hydrogen bonding interacting moiety **S7** has also been introduced to HOF synthesis.[47] Heterosynthons such as pyridine and carboxylic acid **S11** (Figure 4a) have also been used[48] to construct HOFs. Furthermore, charged hydrogen bonding pairs such as guanidium cation and di-, tri-, or tetrasulfonate anion **S12** have been successfully introduced by Ward et al. and others to HOF synthesis.[49−51] The ionic

https://doi.org/10.1021/accountsmr.2c00173
Acc. Mater. Res. XXXX, XXX, XXX−XXX

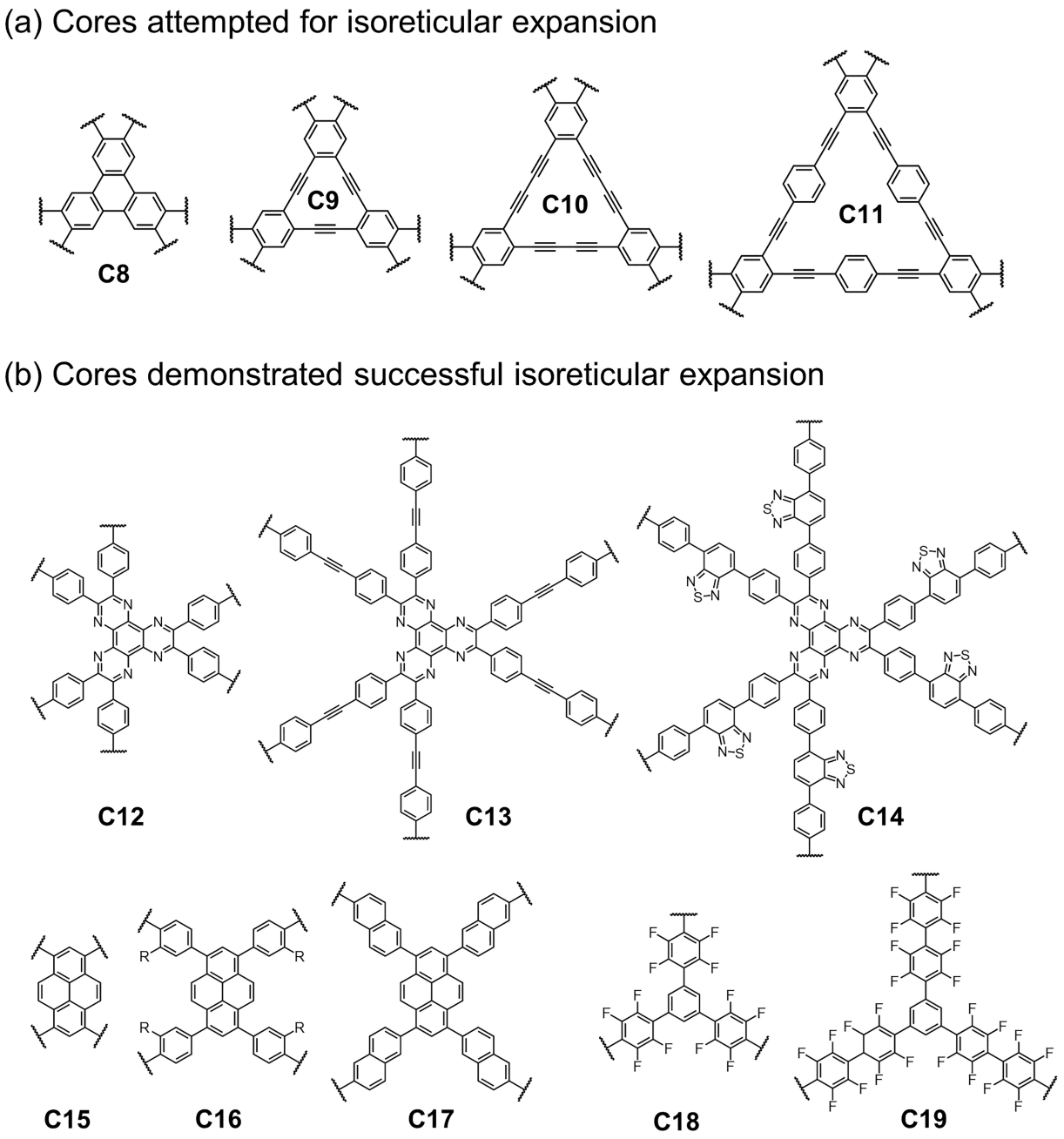

Figure 5. Struts that have been attempted (a) and successfully demonstrated (b) in isoreticularly expanding the pore of HOFs.

interactions and the hydrogen bonding (e.g., **S11**−**S14**) enhance the stability of HOFs. The highly directional and strong hydrogen bonding in this charged pair allows for precise crystal engineering.[49] These hydrogen bonding synthons are also used for the design and synthesis of H_COFs, and their similarities and differences are discussed in Section 4.

While microporous HOFs have been demonstrated efficient for gas separations,[46] expanding the pore size of HOFs is important to absorb larger substrates for separation and catalysis. Isoreticular expansion has been widely used to construct large pore COFs (diameters up to 10 nm).[52] However, this approach faces many problems in HOF construction (similar to H_COFs, discussed later). The molecular building blocks tend to pack more densely in the solid state as different polymorphs. For example, Hisaki et al. synthesized a series of planar π-conjugated molecules with **C8**−**C11** cores and carboxylic acid arms (Figure 5a).[53] Despite the similar geometry and hydrogen bonding, these monomers stacked differently in the solid state. To date, limited success has been made in isoreticularly expanding the pores of HOFs. A C_3-symmetric hexaazatriphenylene[54] **C12** was isoreticularly expanded to **C13** and **C14**,[55] and topologically identical HOFs were obtained with pore sizes increasing from 6 to 20 Å (Figure 5b). Another successful example includes the use of rigid pyrene core **C15** and its derivatives **C16**/**C17**,[56] with the pore sizes of HOFs expanding from 8 × 12 Å to 25 × 30 Å. **S8** and **C18** and **C19** have also been demonstrated for isoreticular expansion of HOFs.[44,45] We share our insights on isoreticular expansion in Section 4. The design of H_COFs requires larger pores because the pore aperture should allow the diffusion of external crosslinker, and the void space of H_COFs synthesized

https://doi.org/10.1021/accountsmr.2c00173
Acc. Mater. Res. XXXX, XXX, XXX−XXX

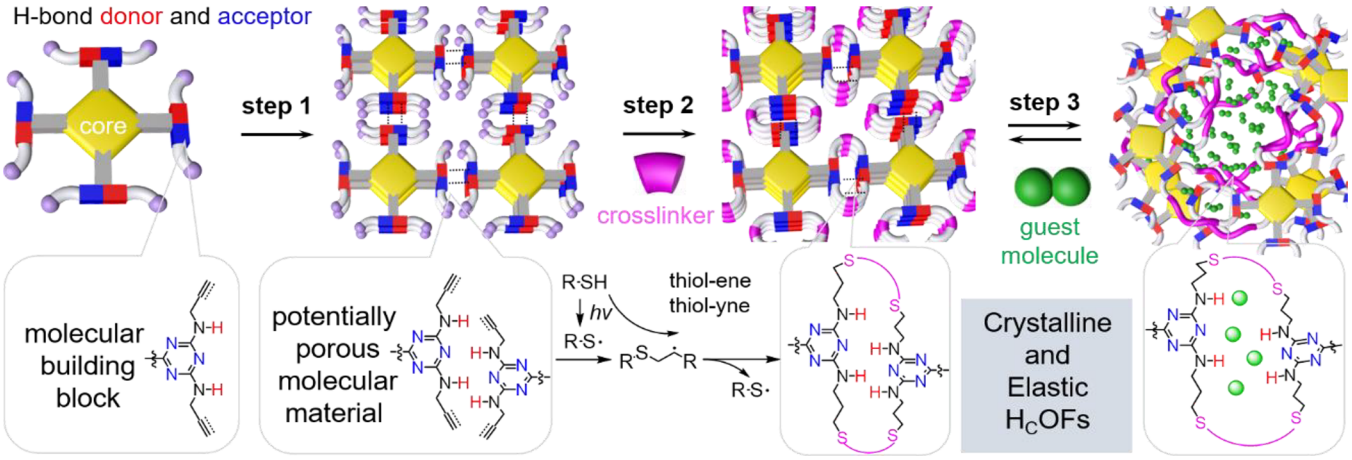

Figure 6. Design of H_COFs through crystallization and subsequent SCSC transformation. Upon guest adsorption, the framework will dynamically change its 3D architecture based on substrate−framework interactions. Reproduced with permission from ref 9. Copyright 2017 American Chemical Society.

after crosslinking is reduced compared to their precursor crystals.

4. HYDROGEN-BONDED CROSSLINKED ORGANIC FRAMEWORKS

Covalently crosslinking preorganized molecular crystals makes it possible to rationally design chemically stable organic materials, a.k.a. H_COFs, with possess periodic, 3D porous networks with high crystallinity. H_COF design drew inspiration from the design of HOFs and COFs (Figure 6). H_COFs have structure similarities to HOFs and COFs; hence, they are anticipated to possess the advantages of both COFs and HOFs. An H_COF monomer consisting of a rigid core, hydrogen bonding arms, and reactive moieties is synthesized and crystallized, forming a precursor crystal. Crosslinkers are diffused into the precursor crystal and undergo photochemical crosslinking to afford the desired H_COF.

While all porous framework materials utilize their defined pore structures to sort guest species by size and shape, some flexible MOFs[57] can dynamically switch their superstructures for highly selective adsorption and separation. Although the framework dynamics in COFs[26] and HOFs are reported,[58] the extent of the organic framework dynamics is very limited due to their rigid covalent or hydrogen bonding connections. H_COFs possess unique guest-responsive dynamics due to their rigid hydrogen-bonded network and flexible crosslinked network. When a strongly binding guest is adsorbed into an H_COF, the hydrogen-bonded network can be disrupted. The network can expand to distances within the allowance of crosslinker extension.

In 2003, Wuest et al. demonstrated the first example[13] of crosslinking a hydrogen-bonded network through diffusion of ethanedithiol $HSCH_2CH_2SH$ (EDT) followed by photoirradiation. The monomer consists of tetraphenylmethane **C6** core and diallylmelamine arms, which crystallized into a hydrogen-bonded network with interconnected helical channels. When EDT was employed as the crosslinker, a stable, covalently crosslinked 3D network was obtained, which retained its crystallinity upon heating to 200 °C. Although this new material was not further investigated until the following decade, it demonstrated the feasibility of achieving long-range order and chemical stability in organic frameworks by covalently crosslinking preorganized molecular crystals.

4.1. Crystal Engineering of H_COF Precursor Crystals

An ideal H_COF precursor crystal should possess continuous large voids for crosslinker diffusion and later substrate sorption, and exposed reactive sites for crosslinking reactions. Appending reactive moieties to reported HOFs could be a starting point, but it is important to take into consideration that the appended reactive groups can often alter the topology of the hydrogen-bonded network.[15] The precursor crystals of H_COFs are not required to possess permanent porosity like HOFs since the covalent crosslinking will stabilize the material. As such, flexible hydrogen-bonded networks that may not survive upon solvent removal could also be utilized in H_COF design. The greater diversity of potential hydrogen-bonded networks marks one of the most distinguishing features between HOFs and H_COF precursor crystals.

In 2017, we synthesized a propargylmelamine-based molecule **M1** (**M** stands for monomer for H_COF, Figure 7a) by attaching four dipropargylmelamines onto a tetraphenylethylene (TPE) core.[9] As a result of the −NH− connection between TPE and propargylmelamine and the noncomplementary hydrogen bonding array of propargylmelamine, **M1** crystallized into a 3D hydrogen-bonded network of *pcu* topology. Later, an allylmelamine-based monomer **M2** was synthesized and crystallized.[14] Despite nearly identical chemical structures shared by **M1** and **M2**, a hydrogen-bonded network of *snw* topology was formed by **M2** with the alternative tilted packing (Figure 7a). In $\mathbf{M1}_{crystal}$ and $\mathbf{M2}_{crystal}$, interconnected voids of 51% and 21% filled with solvent molecules were discovered through SCXRD analysis. The reactive propargyl and allyl groups decorated the pore surfaces, and the neighboring propargyl and allyl groups were 3.3−11.9 Å apart,[9,14] suitable for subsequent thiol−yne and thiol−ene SCSC transformation. Though propargyl/allylmelamine was effective for constructing a large void H_COF precursor crystals, the DAD hydrogen bonding array, multiple potential directions for hydrogen bonding, and rotatable −NH− connections complicate crystal engineering. Network topologies formed by melamine-based monomers are hard to predict.

To increase the directionality and the predictability of the hydrogen-bonded network and reduce the complexity of the crystal engineering, we protonated allylmelamine to allylmelaminium with a DDD hydrogen bonding array.[16] When allylmelaminiums were hydrogen-bonded to a nitrate dimer

https://doi.org/10.1021/accountsmr.2c00173
Acc. Mater. Res. XXXX, XXX, XXX−XXX

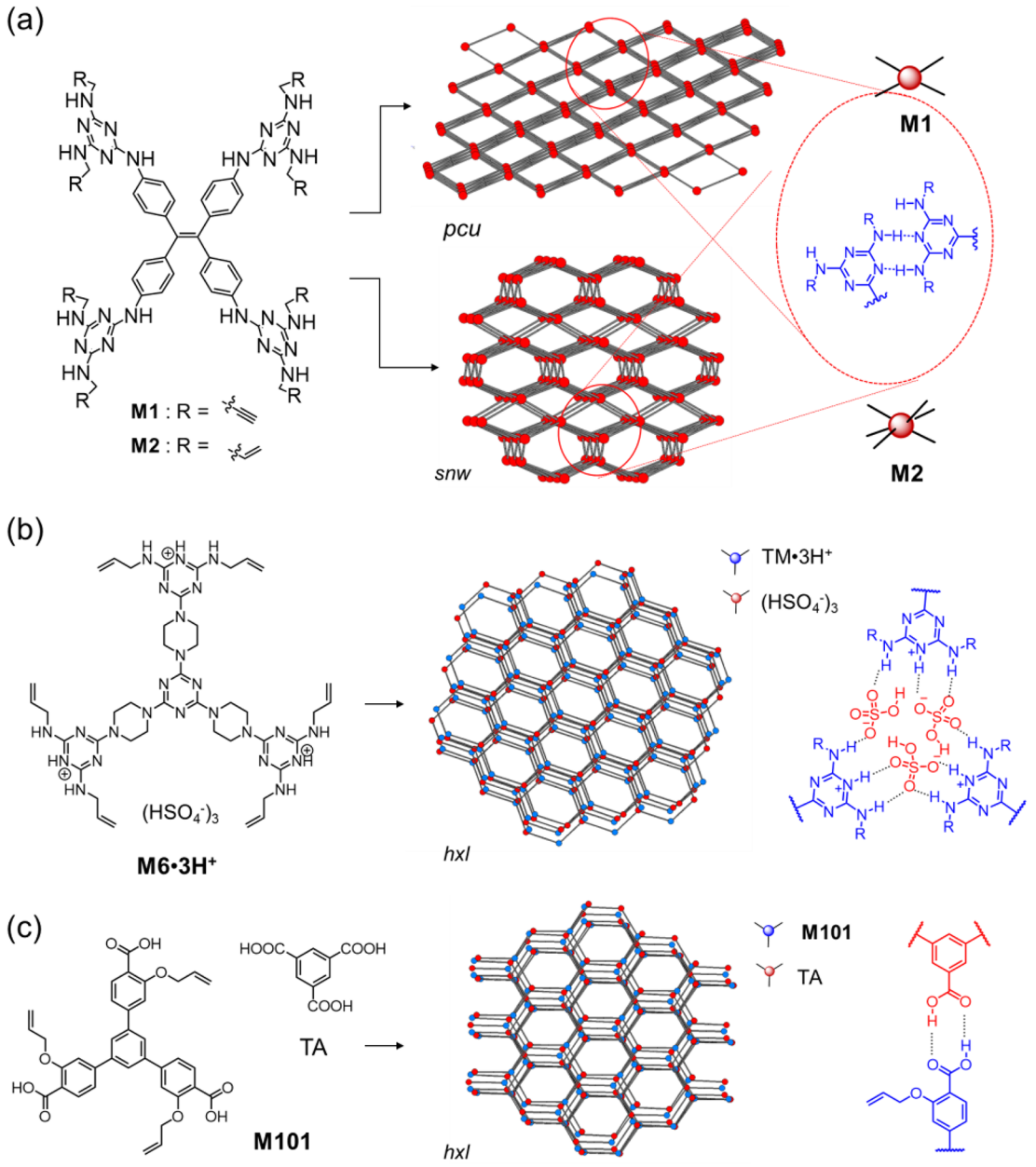

Figure 7. Hydrogen-bonding patterns and topologies of precursor crystals of (a) H_COF-1 and H_COFs-2−4, (b) H_COF-6, and (c) H_COF-101.

$(NO_3^-)_2$ or a bisulfate dimer $(HSO_4^-)_2$, they formed directional, linear hydrogen bonding joints, in which the $(NO_3^-)_2$ or $(HSO_4^-)_2$ acted as dual AAA arrays connecting two melaminium units. The connection is further reinforced by electrostatic interactions between the cationic melaminium and anion dimers. For example, protonated $[\mathbf{M6{\cdot}3H}]^{3+}$ formed solvent-filled hydrogen-bonded networks with nitrate and bisulfate anion clusters (Figure 7b).[16] We discovered that the nitrate anion cluster consists of three nitrate anions and three DMSO, making the joint unstable. $[\mathbf{M6{\cdot}3H}]^{3+}$ formed an *hxl* network with tribisulfate anion clusters $(HSO_4^-)_3$ with large 1D voids (51%) along the *c*-axis with a pore size of 15.3 × 13.8 Å (Figure 7b). Allyl groups pointed toward the pore surface with distances between 2.5 and 11.7 Å, suitable for crosslinking. It is worth noting that the *hxl* network was formed at a higher temperature (~80 °C), and we also obtained a different hydrogen-bonded network formed between $[\mathbf{M6{\cdot}4H}]^{4+}$ and $(HSO_4^-)_4$ at room temperature.

We also introduced carboxylic acid-based monomers for H_COF synthesis[15] since the highly directional $\mathbf{R}_2^2(8)$joints formed by carboxylic acid dimers would direct the assembly of monomers. **M101** was synthesized with three allyl ether groups attached to the *ortho* position of the carboxylic acid moiety (Figure 7c). Not surprisingly, substitution of the *ortho* position of the monomer disrupted the carboxylic acid dimerization in the solid state, common in crystal engineering of carboxylic acid-based monomers. To overcome this problem, we introduced trimesic acid (TA) as a cocrystallization joint. **M101** and TA possess different pK_a values and electron densities at the phenyl moieties, promoting heteromeric carboxylic acid dimerization between **M101** and TA and inhibiting the homodimerization of **M101**. **M101**/TA cocrystallized to form a hexagonal noninterpenetrated large pore network (d = 16 Å), with allyl groups exposed to pore surfaces for crosslinking. We emphasize that, in the **M101** and

https://doi.org/10.1021/accountsmr.2c00173
Acc. Mater. Res. XXXX, XXX, XXX−XXX

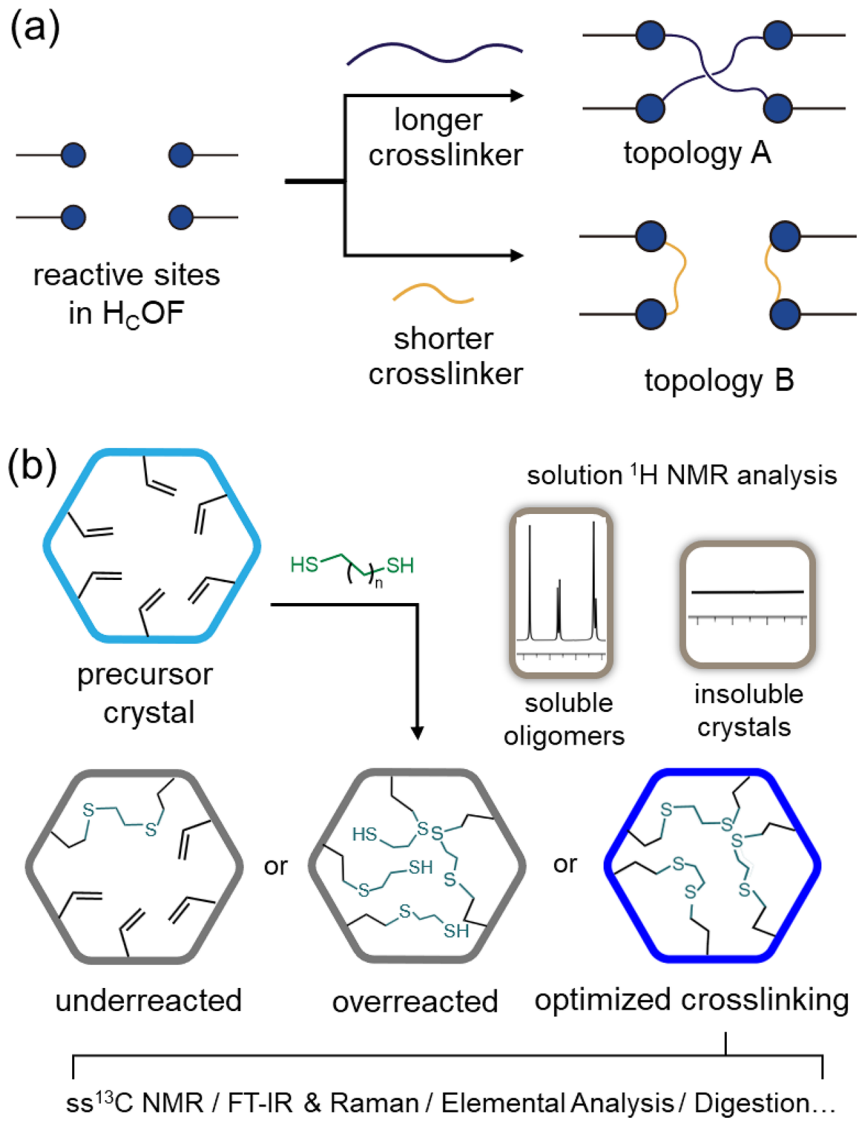

Figure 8. (a) Topochemical crosslinking taking place in a precursor crystal using dithiols of different lengths. (b) Optimization and characterization of H_COFs.

TA cocrystal, **M101** and TA have similar symmetries, but different sizes. Hence, **M101** and TA are packed in an alternating pattern along the *c*-axis, effectively inhibiting the interpenetration of the network. In principle, this approach of employing size-mismatched monomers to form cocrystallized hydrogen-bonded networks provides solutions to address the isoreticular expansion of HOFs and H_COF precursor crystals. Of note is that the alternating stacking of **M101** and TA is not perfectly eclipsed. Such information may be helpful for researchers working in 2D COF structural modeling because most 2D COFs are modeled as perfectly eclipsed or staggered conformations.

4.2. Syntheses of H_COFs

After successful crystallization of the precursor crystals, the next step is to crosslink the reactive sites of the precursor crystals, converting these hydrogen-bonded networks into covalently connected frameworks. Heterogeneously introducing flexible crosslinkers into the voids of the precursor crystal allows for bypassing the strict geometric constraints in topochemical synthesis (see Section 2.2). This method also allows us to employ a variety of flexible building blocks and linking motifs, and a plethora of irreversible reactions that are largely avoided in the current design of COFs. SCXRD analysis of the precursor crystal provides distances between nearby reactive alkenes/alkynes in the crystal lattice, which guides dithiol crosslinker selection. From our experience, EDT is suitable to crosslink the reactive sites between distances of 3.9 and 7 Å, whereas the longer linkers such as propanedithiol (PDT), and butanedithiol (BDT) are suitable for linking propargyl/allyl that are under 8.5 and 10 Å apart, respectively.

Unlike solution phase synthesis, wherein distances between two reactive sites match the length of the crosslinker, H_COF crosslinking reactions can occur between non-neighboring reactive sites in the solid state (Figure 8a). Hence, topologically different H_COFs can be obtained from the same molecular precursor crystals. The divergent H_COF synthesis was illustrated when EDT and PDT were employed to crosslink $\mathbf{M2}_{crystal}$.[14] The olefin motifs in the allyl melamine were distributed along the wide and narrow pore openings in $\mathbf{M2}_{crystal}$, with olefin−olefin distances ranging between 3.5 and 11 Å. When EDT was used as the crosslinker, it stoichiometrically reacted with most nearby allyl groups, converting

https://doi.org/10.1021/accountsmr.2c00173
Acc. Mater. Res. XXXX, XXX, XXX−XXX

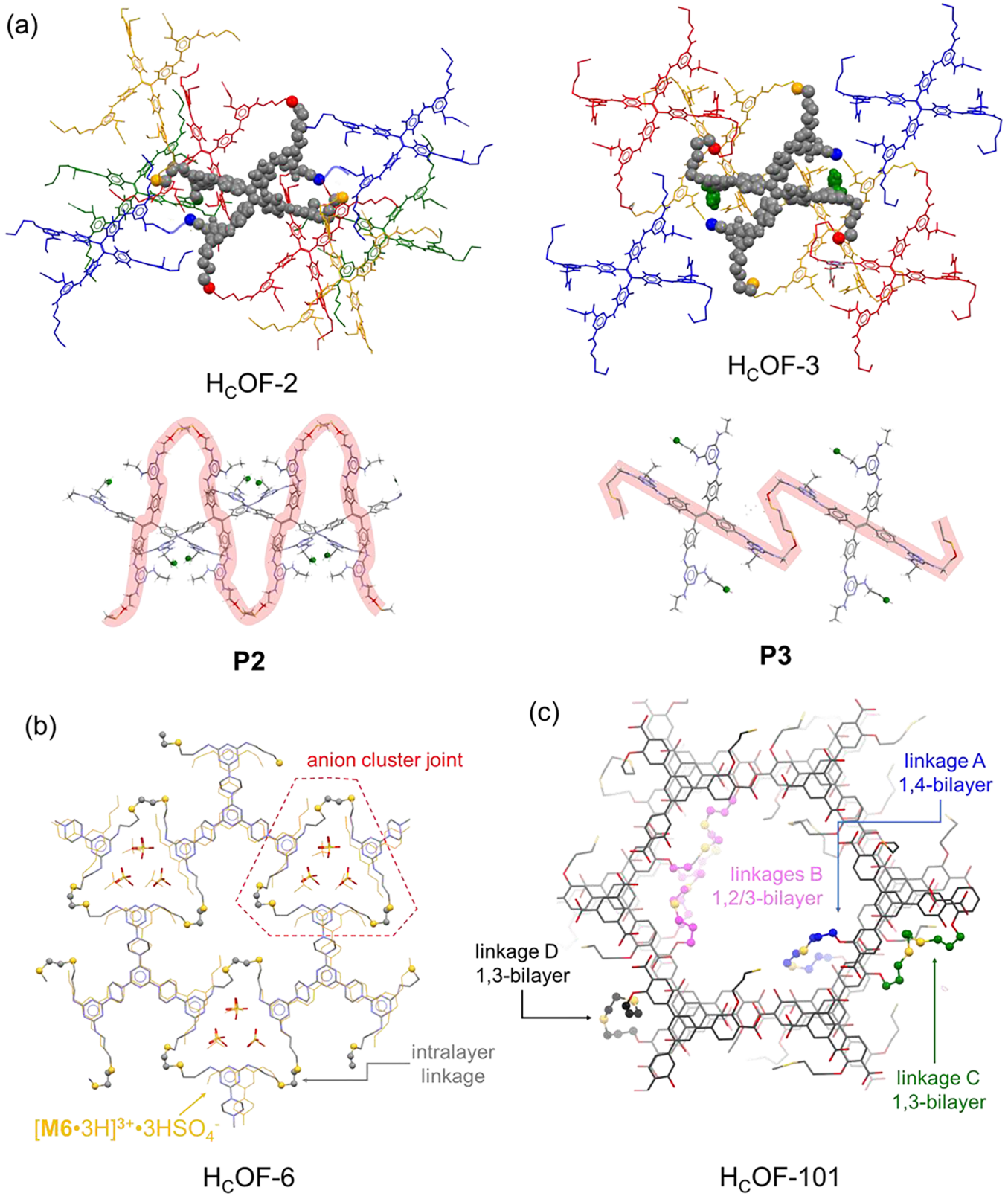

Figure 9. (a) Single-crystal structures of H$_C$OF-2 and **P2** and of H$_C$OF-3 and **P3**. Reproduced with permission from ref 14. Copyright 2019 American Chemical Society. (b) Overlaid single-crystal structures of $[\mathbf{M6{\cdot}3H}]^{3+}{\cdot}\mathbf{3HSO_4}^-$ and H$_C$OF-6. The anion cluster joints of H$_C$OF-6 are highlighted. Reproduced with permission from ref 16. Copyright 2022 Elsevier Inc. (c) Single-crystal structure of H$_C$OF-101 with detailed dithioether linkages connecting different layers. Reproduced with permission from ref 15. Copyright 2021 John Wiley & Sons, Inc.

them to the dithioethers in H$_C$OF-2. When PDT was employed, six of eight allyl groups reacted, leaving two olefins in the more congested areas unreacted.

When the pore aperture of the precursor crystal is expanded, the use of higher crosslinker concentrations may result in overreaction (with unreacted thiols) and significantly reduce

https://doi.org/10.1021/accountsmr.2c00173
Acc. Mater. Res. XXXX, XXX, XXX−XXX

the crosslinking degree of H_COFs (Figure 8b). This overreaction was observed during the synthesis of H_COF-6 (pore diameter ~15 Å)[16] and H_COF-101 (pore diameter ~16 Å),[15] when overreaction afforded products soluble in hot DMF and DMSO that could be monitored using ^{1}H NMR spectroscopy. On the other hand, underreacted products obtained from dilute dithiol solutions are also soluble for ^{1}H NMR analysis (Figure 8b). Therefore, reducing the soluble species to a minimum by adjusting crosslinker concentrations is the first step in the optimization of the H_COF synthesis. The chemical compositions of the synthesized crystals need to be thoroughly characterized before SCXRD analysis. After photo-crosslinking, FT-IR and Raman spectroscopy analyses reveal whether free thiols exist. Solid-state ^{13}C NMR spectroscopy is used to confirm the consumption of allyl/propargyl groups and the formation of thioethers. Elemental analysis is important for the composition analysis of H_COFs. The experimentally measured weight percentages of C/H/N/S elements of a synthetically well-optimized H_COF are found within 0.5 wt % of the theoretical values, similar to the accuracy of small molecule elemental analysis. We also introduced a digestion method to confirm the composition of H_COF-101 by hydrolyzing the framework into soluble species for ^{1}H NMR analysis. After confirming the chemical composition of the synthesized H_COFs, high-quality single-crystal samples are prepared for SCXRD analysis.

4.3. SCXRD Analysis of H_COFs

A well-refined H_COF structure is critical for determining structure−property relationships. While the SCXRD data collection for H_COF precursor crystals is usually performed at in-house diffractometers, crosslinked H_COFs often require high energy synchrotron radiation due to reduced crystal quality after SCSC. During data refinement, the rigid hydrogen-bonded networks of H_COFs are often modeled without any ambiguity, though the dithioether linkages may adopt several positions in a H_COF. Thus, several disordered linkages need to be modeled. During the structural analysis of H_COFs, we have encountered different challenges in SCXRD analysis and developed several methods to overcome these challenges, which we describe below case by case. We emphasize that small molecule crystallography standards (e.g., R_1 < 10%) are not suitable for evaluating the crystal data quality of H_COFs, since these networks are large and possess significant disordered parts. Those atoms still diffract but may not contribute to discrete diffraction points. Instead, standards similar to macromolecular crystallography analysis (e.g., R ~ 20−30%) should be considered.[59]

H_COF-1.[9] Due to the high number of disordered flexible dithioether linkages as well as the randomly generated stereogenic centers after crosslinking, the quality of the X-ray diffraction data was too poor for SCXRD analysis. Only the unit cell parameters were reported, and the crosslinked structure was obtained through simulation using unit cell parameter and PXRD data.

H_COFs-2 and -3.[14] The hydrogen-bonded networks of H_COFs-2 and -3 were found to be very similar to the structure of the precursor crystal $\mathbf{M2}_{crystal}$. The assignment of four out of eight dithioether linkages was straightforward with disordered atoms modeled over several positions. Due to the weak and smeared electron density, atomic placements of the other four dithioether linkages were ambiguous based on SCXRD data of H_COFs-2 and -3 alone. Therefore, we synthesized two analogous polymers **P2** (**P** stands for polymers in H_COF synthesis) and **P3**, by reducing the number of dithioether linkages on each DAT moiety from two to one. The resolved SCXRD structures of **P2** and **P3** (Figure 9a) not only confirmed the correct atomic placements of the four modeled-in linkages but also provided important structural guidance for the modeling of the other four linkages. Furthermore, we performed a two-step reaction on the precursor crystal of H_COFs-2 and -3 using ethanethiol first to consume four allyl groups in each **M2**, and then crosslinking the remaining four allyl groups using EDT. Combining the SCXRD analysis of H_COFs-2 and -3, **P2-3**, and two-step reaction outcomes, the network structures of H_COF-2 and H_COF-3 were determined unambiguously (Figure 9a). H_COF-2 was found as a new, 3-nodal 3,3,4-connected self-entangled 3D network (*cdc*, named after Chemistry Dartmouth College), whereas H_COF-3 was found as a 2D 3,4-connected bilayer network.

H_COF-6.[16] The precursor crystal $[\mathbf{M6{\cdot}3H}]^{3+}{\cdot}3HSO_4^-$ diffracted weakly, and the quality of the diffraction was further reduced in H_COF-6 after crosslinking. Surprisingly, data of reasonable quality were collected using an Mo-radiation source with an extended exposure time. The backbone of H_COF-6 and $(HSO_4^-)_3$ anion cluster were resolved in a straightforward manner (Figure 9b). Smeared electron densities attributed to dithioether linkages were distributed near the backbone, making the atomic placement ambiguous. To assist the SCXRD analysis, we experimentally swelled H_COF-6 in phenol and found that this crystal expanded more than 2.5 times along the *c*-axis and shrunk slightly along the *a*/*b* plane. We also set up hypothetical models of H_COF-6 within molecular dynamics (MD) simulations with varying proportions of crosslinking assigned as inter- vs intralayer. Only models with over 67% of crosslinking assigned as intralayer could match experimental observations. Thus, a representative crystal structure of H_COF-6 possessing 100% intralayer linkages was modeled (Figure 9b), although we do acknowledge the existence of a small percentage of interlayer crosslinks as defects.

H_COF-101.[15] The allyl groups in the $\mathbf{M101}/TA_{crystal}$ cocrystal were disordered over two positions with equal probabilities on either side of the phenyl rings of **M101**. After crosslinking, the formed dithioether linkages in H_COF-101 reduced the symmetry of the crystal and changed its unit cell compared to that of the cocrystal. The rigid hydrogen-bonded network of H_COF-101 was found near identical to the precursor cocrystal. Luckily, synchrotron data provided sufficient electron densities to model dithioether linkages, some of which were overlapped. Refinement of the H_COF-101 revealed the formation of a 3D crosslinked network featuring a pore diameter of 14 Å, with crosslinking between 1,2-, 1,3-, and 1,4-layers (Figure 9c). The void space of H_COF-101 is calculated as 27% using the refined single-crystal X-ray structure.

4.4. Dynamic Sorption of H_COFs

The periodically distributed voids in H_COFs can be activated upon solvent removal. After supercritical CO_2 activation and high vacuum, H_COFs remained highly crystalline, as shown in PXRD analysis.[9,14−16] The permanent porosity of H_COFs was examined using N_2, CO_2, H_2O, and other organic solvent vapor sorption isotherms. H_COFs showed low CO_2 uptakes at room temperature and negligible N_2 adsorptions.[9,14−16] The causes of the low N_2 and CO_2 adsorptions of H_COFs is still unclear, but similar phenomena were also observed in many

https://doi.org/10.1021/accountsmr.2c00173
Acc. Mater. Res. XXXX, XXX, XXX−XXX

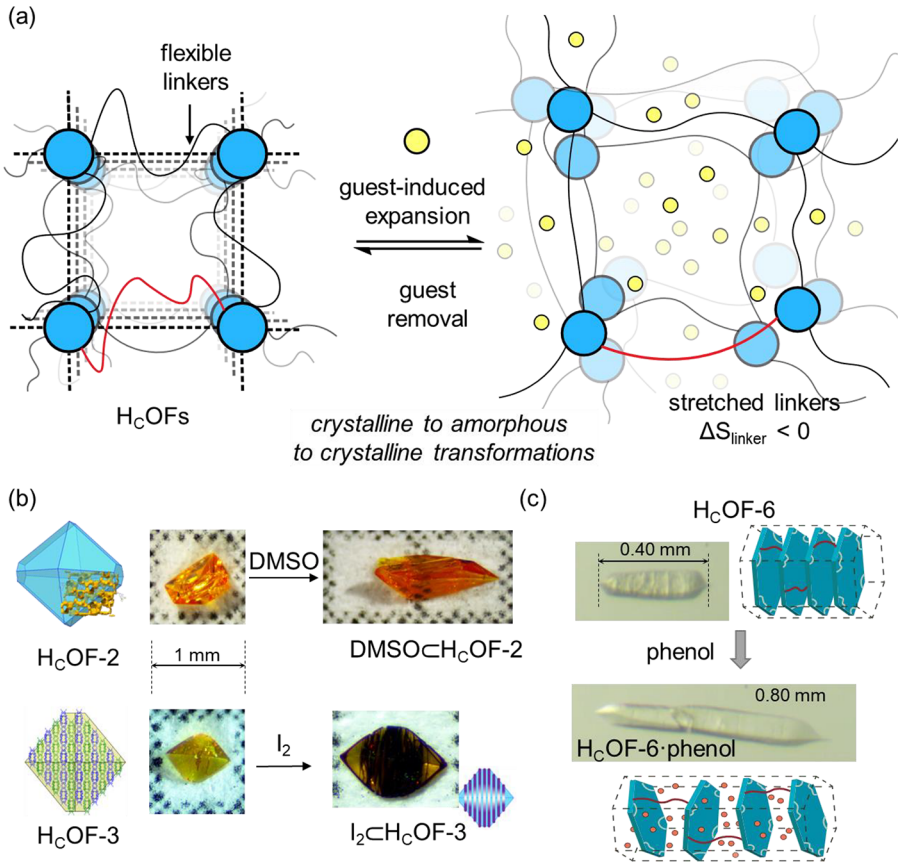

Figure 10. (a) Graphical illustration of the dynamic sorption of H_COFs upon disrupting and re-forming hydrogen-bonded networks. (b) Crystal size expansion of H_COFs-2 and -3 upon guest uptake. Reproduced with permission from ref 14. Copyright 2019 American Chemical Society. (c) Images and illustrations of the expansion of H_COF-6 upon phenol uptake. Reproduced with permission from ref 16. Copyright 2022 Elsevier Inc.

HOFs.[8,36,37] Therefore, vapor sorption isotherms were measured to demonstrate the permanent porosity of H_COFs. For example, H_COF-101 showed good vapor uptake of water, methanol, and toluene at 91, 92, and 105 $cm^3\ g^{-1}$ at 24 °C, respectively.[15] Similar vapor uptake values were measured using H_COF-6.[16] After vapor sorption analysis, the crystallinity of H_COFs remained, as shown in PXRD analysis.[15,16]

The combination of flexible covalent linkages and rigid hydrogen-bonding networks endow H_COFs with unique dynamic guest sorption properties (Figure 10a). When strongly binding guests enter the permanent voids of H_COFs, they disrupt the hydrogen bonding networks of H_COF, resulting in the expansion of H_COF materials, losing long-range order (i.e., crystallinity). The flexible crosslinkers are stretched upon expansion (entropy loss) and the extent of expansion is dependent on the crosslinkers' lengths and densities. These stretched crosslinkers keep the short-range order of the expanded H_COFs. The guest adsorption-induced size expansion of H_COFs is similar to the swelling of crosslinked polymers. When guests are desorbed from the framework, the conformation recovery of flexible linkages provides favorable entropy incentives, along with enthalpy regained from the re-formation of the hydrogen-bonded framework, enabling the framework to regain crystallinity. Depending on the extent of the expansion and the binding energy of the framework-to-substrate, the expansion and contraction of H_COFs are not always fully reversible.

Iodine (I_2) forms halogen bonding interactions with melamine moieties and activates the dormant voids (in addition to the permanent voids) of H_COFs. H_COFs-1−4 showed remarkable I_2 adsorption capacities of 2.1−3.6 g/g in an aqueous environment. Macroscopically, the crystal of H_COF-2 showed visible size expansion to more than twice its original size (Figure 10b). The iodine adsorption-induced crystal size expansion was anisotropic, and the most extended direction indicates the lowest density of crosslinking. For example, H_COF-3 crystals showed an exfoliation-of-bilayer-like expansion upon I_2 uptake. Hence, the macroscale size expansion also provides indirect network architecture information in H_COFs. The calculated van der Waals volume of adsorbed I_2 exceeded the available void space of H_COF-2 and H_COF-3 by 473% and 668% due to the elastic expansion of the framework during adsorption. The high-capacity adsorption of iodine in the aqueous environment, along with the good chemical stability of H_COFs, enables the potential use of these materials for radioactive iodine removal or water treatment. We found that DMSO is also effective in activating the dormant voids of H_COFs, morphing them into less isotropic, amorphous materials (Figure 10b).

Due to the multivalent hydrogen bonding network, only strongly binding guests can activate the dormant voids of melamine-based H_COFs. This feature, on one hand, significantly enhanced the substrate selectivity but, on the other hand, limited the substrate scope. To this end, the anion-cluster-based H_COF-6 was synthesized. The electrostatic repulsion between bisulfate anions in H_COF-6 requires a smaller energy penalty for the disruption of the hydrogen-bonded network to trigger the expansion of H_COFs. Phenol

https://doi.org/10.1021/accountsmr.2c00173
Acc. Mater. Res. XXXX, XXX, XXX−XXX

and its analogues demonstrated their capability to expand the size of H_COF-6 crystal (Figure 10c) during adsorption by disrupting the anion clusters. Multicycle crystal size expansions and contractions were found when H_COF-6 adsorb and desorb phenols. In H_COF-101, the disruption of the hydrogen-bonded network of H_COF-101 resulted in the loss of TA in hot DMSO, since TA was not covalently crosslinked to the framework.

5. OUTLOOK AND FUTURE DIRECTIONS

This Account summarizes approaches to construct single-crystalline hydrogen-bonded crosslinked framework materials and analogous framework materials, including COFs and HOFs. The porous nature of these materials makes them promising for various applications, and the atomic-level understanding of the framework architecture and the local environment for framework−guest interaction reveals important fundamental insights to establish structure−property relationships. Moving forward, the development of electron diffraction techniques has significantly accelerated the discovery of single-crystalline COFs. With more researchers having access to such techniques, the structure elucidations of 2D polymers, HOFs, and H_COFs are expected to be expedited. Undeniably, the crystal engineering of the precursor crystals of H_COFs is not straightforward. It is reasonable to be optimistic that the rapid growth of the HOF materials will inform H_COF precursors' crystal engineering and accelerate the discovery of H_COF materials. Recently, machine-learning-based computational prediction of crystal packing showed exciting progress,[58,60] which could be expanded to porous molecular crystal packing predictions in the foreseeable future.

Expanding the toolbox of H_COF synthesis and introducing other reactions for SCSC transformations will also expand the family of H_COFs. Candidate reactions such as [2 + 2] cycloaddition and diacetylene polymerization should be considered for future H_COF design. Polymerization reactions that are incompatible with most COF syntheses, such as free-radical polymerization, olefin metathesis, and cationic/anionic ring opening polymerization commonly used for conventional polymer synthesis, could also be introduced for H_COFs, highlighting the unique solid-state chemical environments of H_COF. The guest-induced elastic expansion of H_COFs makes them unique among other crystalline organic framework materials. The elastic nature of H_COF crystals will compensate for the entropy loss during the absorption of guests and give rise to high capacities. Moreover, H_COFs have the potential to expand the traditional sorption mechanism based on size-sieving. More studies are necessary to expand the currently small library of reported guests and exploit the potential of H_COF materials as tools for catalysis and separation with low energy consumption.

AUTHOR INFORMATION

Corresponding Author

Chenfeng Ke − *Department of Chemistry, Dartmouth College, Hanover, New Hampshire 03755, United States;* orcid.org/0000-0002-4689-8923; Email: chenfeng.ke@dartmouth.edu

Authors

Jayanta Samanta − *Department of Chemistry, Dartmouth College, Hanover, New Hampshire 03755, United States*

Yunjia Zhang − *Department of Chemistry, Dartmouth College, Hanover, New Hampshire 03755, United States*

Mingshi Zhang − *Department of Chemistry, Dartmouth College, Hanover, New Hampshire 03755, United States*

Albert D. Chen − *Department of Chemistry, Dartmouth College, Hanover, New Hampshire 03755, United States;* orcid.org/0000-0002-1865-4673

Complete contact information is available at: https://pubs.acs.org/10.1021/accountsmr.2c00173

Author Contributions

†J.S and Y.Z. contributed equally.

Notes

The authors declare no competing financial interest.

Biographies

Jayanta Samanta is a research associate in the laboratory of Prof. Chenfeng Ke at Dartmouth College. He received his B.Sc. and M.Sc. in chemistry from Vidyasagar University, India, and Ph.D. in supramolecular chemistry from the CSIR-Indian Institute of Chemical Biology, India, under the supervision of Dr. Ramalingam Natarajan. His current research focuses on developing H_COF materials and studying their dynamic behaviors.

Yunjia Zhang is a Ph.D. candidate under the supervision of Prof. Chenfeng Ke at Dartmouth College. He received his B.S. degree from Fudan University (China) in 2020. His research interests mainly focus on the design and construction of H_COFs.

Mingshi Zhang is a Ph.D. candidate under the supervision of Prof. Chenfeng Ke at Dartmouth College. He mainly works on developing H_COF materials and 3D-printing porous organic materials. He received his B.S. degree from Nankai University in 2017.

Albert D. Chen currently is a graduate student in the Department of Chemistry at Columbia University. He was an undergraduate researcher under the supervision of Prof. Chenfeng Ke at Dartmouth College (2019−2022). He completed his Senior Research Fellowship major thesis focusing on the development of novel methods for the synthesis of H_COFs.

Chenfeng Ke is an Associate Professor in the Department of Chemistry at Dartmouth College. He obtained his B.S. and Ph.D. from the College of Chemistry, Nankai University, in 2004 and 2009, respectively. He worked with Prof. Anthony Davis at the University of Bristol (2009−2011, Newton fellow, Royal Society) and Sir Fraser Stoddart at Northwestern University (2011−2015), before taking the current faculty position at Dartmouth College (2015 to present). His research focuses on developing smart materials for 3D printing applications, elastic crystalline porous organic materials for energy and environmental-related applications, and carbohydrate receptors for biological recognition and sensing.

ACKNOWLEDGMENTS

This work is jointly supported by the National Science Foundation CAREER award (DMR 1844920), the Arnold and Mabel Beckman Foundation Beckman Young Investigator program, the American Chemical Society Petroleum Research Fund (58377-DNI10), the G. Norman Albree Trust Fund from the Bank of America, and NSF EPSCoR-1757371 to C.K.

REFERENCES

(1) Slater, A. G.; Cooper, A. I. Function-Led Design of New Porous Materials. *Science* **2015**, *348*, aaa8075.

(2) Islamoglu, T.; Chen, Z. J.; Wasson, M. C.; Buru, C. T.; Kirlikovali, K. O.; Afrin, U.; Mian, M. R.; Farha, O. K. Metal-Organic Frameworks against Toxic Chemicals. *Chem. Rev.* **2020**, *120*, 8130−8160.
(3) Shi, J.; Wang, Y.; Yang, W.; Tang, Y.; Xie, Z. Recent Advances of Pore System Construction in Zeolite-Catalyzed Chemical Industry Processes. *Chem. Soc. Rev.* **2015**, *44*, 8877−8903.
(4) Li, W.; Liu, J.; Zhao, D. Y. Mesoporous Materials for Energy Conversion and Storage Devices. *Nat. Rev. Mater.* **2016**, *1*, 16023.
(5) Kuppler, R. J.; Timmons, D. J.; Fang, Q. R.; Li, J. R.; Makal, T. A.; Young, M. D.; Yuan, D.; Zhao, D.; Zhuang, W.; Zhou, H. C. Potential Applications of Metal-Organic Frameworks. *Coord. Chem. Rev.* **2009**, *253*, 3042−3066.
(6) Yaghi, O. M.; Kalmutzki, M. J.; Diercks, C. S.*Introduction to Reticular Chemistry: Metal-Organic Frameworks and Covalent Organic Frameworks*; John Wiley & Sons, 2019.
(7) Geng, K. Y.; He, T.; Liu, R. Y.; Dalapati, S.; Tan, K. T.; Li, Z. P.; Tao, S. S.; Gong, Y. F.; Jiang, Q. H.; Jiang, D. L. Covalent Organic Frameworks: Design, Synthesis, and Functions. *Chem. Rev.* **2020**, *120*, 8814−8933.
(8) Lin, R.; Chen, B. Hydrogen-Bonded Organic Frameworks: Chemistry and Functions. *Chem.* **2022**, *8*, 2114−2135.
(9) Lin, Y. X.; Jiang, X. F.; Kim, S. T.; Alahakoon, S. B.; Hou, X.; Zhang, Z. Y.; Thompson, C. M.; Smaldone, R. A.; Ke, C. An Elastic Hydrogen-Bonded Cross-Linked. Organic Framework for Effective Iodine Capture in Water. *J. Am. Chem. Soc.* **2017**, *139*, 7172−7175.
(10) Ma, T. Q.; Kapustin, E. A.; Yin, S. X.; Liang, L.; Zhou, Z. Y.; Niu, J.; Li, L. H.; Wang, Y. Y.; Su, J.; Li, J.; Wang, X. G.; Wang, W. D.; Wang, W.; Sun, J. L.; Yaghi, O. M. Single-Crystal X-Ray Diffraction Structures of Covalent Organic Frameworks. *Science* **2018**, *361*, 48−52.
(11) Beaudoin, D.; Maris, T.; Wuest, J. D. Constructing Monocrystalline Covalent Organic Networks by Polymerization. *Nat. Chem.* **2013**, *5*, 830−834.
(12) Huang, Z. H.; Grape, E. S.; Li, J.; Inge, A. K.; Zou, X. D. 3D Electron Diffraction as an Important Technique for Structure Elucidation of Metal-Organic Frameworks and Covalent Organic Frameworks. *Coord. Chem. Rev.* **2021**, *427*, 213583.
(13) Brunet, P.; Demers, E.; Maris, T.; Enright, G. D.; Wuest, J. D. Designing Permeable Molecular Crystals That React with External Agents to Give Crystalline Products. *Angew. Chem. Int. Ed* **2003**, *42*, 5303−5306.
(14) Jiang, X. F.; Cui, X. Z.; Duncan, A. J. E.; Li, L.; Hughes, R. P.; Staples, R. J.; Alexandrov, E. V.; Proserpio, D. M.; Wu, Y. Y.; Ke, C. Topochemical Synthesis of Single-Crystalline Hydrogen-Bonded Cross-Linked Organic Frameworks and Their Guest-Induced Elastic Expansion. *J. Am. Chem. Soc.* **2019**, *141*, 10915−10923.
(15) Liang, R.; Samanta, J.; Shao, B.; Zhang, M.; Staples, R. J.; Chen, A. D.; Tang, M.; Wu, Y.; Aprahamian, I.; Ke, C. A Heteromeric Carboxylic Acid Based Single-Crystalline Crosslinked Organic Framework. *Angew. Chem. Int. Ed.* **2021**, *60*, 23176−23181.
(16) Samanta, J.; Dorn, R. W.; Zhang, W. L.; Jiang, X. F.; Zhang, M. S.; Staples, R. J.; Rossini, A. J.; Ke, C. An Ultra-Dynamic Anion-Cluster-Based Organic Framework. *Chem.* **2022**, *8*, 253−267.
(17) Schlüter, A. D.; Weber, T.; Hofer, G. How to Use X-Ray Diffraction to Elucidate 2D Polymerization Propagation in Single Crystals. *Chem. Soc. Rev.* **2020**, *49*, 5140−5158.
(18) Côté, A. P.; Benin, A. I.; Ockwig, N. W.; O'Keeffe, M.; Matzger, A. J.; Yaghi, O. M. Porous, Crystalline, Covalent Organic Frameworks. *Science* **2005**, *310*, 1166−1170.
(19) Smith, B. J.; Dichtel, W. R. Mechanistic Studies of Two-Dimensional Covalent Organic Frameworks Rapidly Polymerized from Initially Homogenous Conditions. *J. Am. Chem. Soc.* **2014**, *136*, 8783−8789.
(20) Evans, A. M.; Parent, L. R.; Flanders, N. C.; Bisbey, R. P.; Vitaku, E.; Kirschner, M. S.; Schaller, R. D.; Chen, L. X.; Gianneschi, N. C.; Dichtel, W. R. Seeded Growth of Single-Crystal Two-Dimensional Covalent Organic Frameworks. *Science* **2018**, *361*, 52−57.
(21) Kandambeth, S.; Mallick, A.; Lukose, B.; Mane, M. V.; Heine, T.; Banerjee, R. Construction of Crystalline 2D Covalent Organic Frameworks with Remarkable Chemical (Acid/Base) Stability via a Combined Reversible and Irreversible Route. *J. Am. Chem. Soc.* **2012**, *134*, 19524−19527.
(22) Dalapati, S.; Jin, S. B.; Gao, J.; Xu, Y. H.; Nagai, A.; Jiang, D. L. An Azine-Linked Covalent Organic Framework. *J. Am. Chem. Soc.* **2013**, *135*, 17310−17313.
(23) Feriante, C.; Evans, A. M.; Jhulki, S.; Castano, I.; Strauss, M. J.; Barlow, S.; Dichtel, W. R.; Marder, S. R. New Mechanistic Insights into the Formation of Imine-Linked Two-Dimensional Covalent Organic Frameworks. *J. Am. Chem. Soc.* **2020**, *142*, 18637−18644.
(24) Zhang, Y. B.; Su, J.; Furukawa, H.; Yun, Y. F.; Gándara, F.; Duong, A.; Zou, X. D.; Yaghi, O. M. Single-Crystal Structure of a Covalent Organic Framework. *J. Am. Chem. Soc.* **2013**, *135*, 16336−16339.
(25) Ma, T. Q.; Li, J.; Niu, J.; Zhang, L.; Etman, A. S.; Lin, C.; Shi, D. E.; Chen, P. H.; Li, L. H.; Du, X.; Sun, J. L.; Wang, W. Observation of Interpenetration Isomerism in Covalent Organic Frameworks. *J. Am. Chem. Soc.* **2018**, *140*, 6763−6766.
(26) Sun, T.; Wei, L.; Chen, Y. C.; Ma, Y. H.; Zhang, Y. B. Atomic-Level Characterization of Dynamics of a 3D Covalent Organic Framework by Cryo-Electron Diffraction Tomography. *J. Am. Chem. Soc.* **2019**, *141*, 10962−10966.
(27) Sun, T.; Hughes, C. E.; Guo, L. S.; Wei, L.; Harris, K. D. M.; Zhang, Y. B.; Ma, Y. H. Direct-Space Structure Determination of Covalent Organic Frameworks from 3D Electron Diffraction Data. *Angew. Chem. Int. Ed* **2020**, *59*, 22638−22644.
(28) Hema, K.; Ravi, A.; Raju, C.; Pathan, J. R.; Rai, R.; Sureshan, K. M. Topochemical Polymerizations for the Solid-State Synthesis of Organic Polymers. *Chem. Soc. Rev.* **2021**, *50*, 4062−4099.
(29) Schmidt, G. Photodimerization in the Solid State. *Pure Appl. Chem.* **1971**, *27*, 647−678.
(30) Sun, C.; Oppenheim, J. J.; Skorupskii, G.; Yang, L.; Dincă, M. Reversible Topochemical Polymerization and Depolymerization of a Crystalline 3D Porous Organic Polymer with C−C Bond Linkages. *Chem.* **2022**, DOI: 10.1016/j.chempr.2022.07.028.
(31) Lange, R. Z.; Hofer, G.; Weber, T.; Schlüter, A. D. A Two-Dimensional Polymer Synthesized through Topochemical [2 + 2]-Cycloaddition on the Multigram Scale. *J. Am. Chem. Soc.* **2017**, *139*, 2053−2059.
(32) Kissel, P.; Erni, R.; Schweizer, W. B.; Rossell, M. D.; King, B. T.; Bauer, T.; Götzinger, S.; Schlüter, A. D.; Sakamoto, J. A Two-Dimensional Polymer Prepared by Organic Synthesis. *Nat. Chem.* **2012**, *4*, 287−291.
(33) Kory, M. J.; Wörle, M.; Weber, T.; Payamyar, P.; van de Poll, S. W.; Dshemuchadse, J.; Trapp, N.; Schlüter, A. D. Gram-Scale Synthesis of Two-Dimensional Polymer Crystals and Their Structure Analysis by X-Ray Diffraction. *Nat. Chem.* **2014**, *6*, 779−784.
(34) Kissel, P.; Murray, D. J.; Wulftange, W. J.; Catalano, V. J.; King, B. T. A Nanoporous Two-Dimensional Polymer by Single-Crystal-to-Single-Crystal Photopolymerization. *Nat. Chem.* **2014**, *6*, 774−778.
(35) Yelgaonkar, S. P.; Campillo-Alvarado, G.; MacGillivray, L. R. Phototriggered Guest Release from a Nonporous Organic Crystal: Remarkable Single-Crystal-to-Single-Crystal Transformation of a Binary Cocrystal Solvate to a Ternary Cocrystal. *J. Am. Chem. Soc.* **2020**, *142*, 20772−20777.
(36) Lin, R. B.; He, Y.; Li, P.; Wang, H.; Zhou, W.; Chen, B. Multifunctional Porous Hydrogen-Bonded Organic Framework Materials. *Chem. Soc. Rev.* **2019**, *48*, 1362−1389.
(37) Song, X.; Wang, Y.; Wang, C.; Wang, D.; Zhuang, G.; Kirlikovali, K. O.; Li, P.; Farha, O. K. Design Rules of Hydrogen-Bonded Organic Frameworks with High Chemical and Thermal Stabilities. *J. Am. Chem. Soc.* **2022**, *144*, 10663−10687.
(38) Li, P.; Ryder, M. R.; Stoddart, J. F. Hydrogen-Bonded Organic Frameworks: A Rising Class of Porous Molecular Materials. *Acc. Mater. Res.* **2020**, *1*, 77−87.

https://doi.org/10.1021/accountsmr.2c00173
Acc. Mater. Res. XXXX, XXX, XXX−XXX

(39) Duchamp, D. J.; Marsh, R. E. The Crystal Structure of Trimesic Acid (Benzene-1, 3, 5-Tricarboxylic Acid). *Acta Crystallogr. Sect. B* **1969**, *25*, 5−19.
(40) Simard, M.; Su, D.; Wuest, J. D. Use of Hydrogen Bonds to Control Molecular Aggregation. Self-Assembly of Three-Dimensional Networks with Large Chambers. *J. Am. Chem. Soc.* **1991**, *113*, 4696−4698.
(41) Brunet, P.; Simard, M.; Wuest, J. D. Molecular Tectonics. Porous Hydrogen-Bonded Networks with Unprecedented Structural Integrity. *J. Am. Chem. Soc.* **1997**, *119*, 2737−2738.
(42) He, Y.; Xiang, S.; Chen, B. A Microporous Hydrogen-Bonded Organic Framework for Highly Selective C_2H_2/C_2H_4 Separation at Ambient Temperature. *J. Am. Chem. Soc.* **2011**, *133*, 14570−14573.
(43) Zhang, M. S.; Samanta, J.; Ke, C. Assembling Guests as Cyclic Tetramers in a Porous Hydrogen-Bonded Organic Framework. *Cryst. Growth Des* **2022**, *22*, 3421−3427.
(44) Chen, T. H.; Popov, I.; Kaveevivitchai, W.; Chuang, Y. C.; Chen, Y. S.; Daugulis, O.; Jacobson, A. J.; Miljanić, O. Š. Thermally Robust and Porous Noncovalent Organic Framework with High Affinity for Fluorocarbons and CFCs. *Nat. Commun.* **2014**, *5*, 5131.
(45) Hashim, M. I.; Le, H. T. M.; Chen, T. H.; Chen, Y. S.; Daugulis, O.; Hsu, C. W.; Jacobson, A. J.; Kaveevivitchai, W.; Liang, X.; Makarenko, T.; Miljanić, O. Š.; Popovs, I.; Tran, H. V.; Wang, X.; Wu, C. H.; Wu, J. I. Dissecting Porosity in Molecular Crystals: Influence of Geometry, Hydrogen Bonding, and $[\pi\cdots\pi]$ Stacking on the Solid-State Packing of Fluorinated Aromatics. *J. Am. Chem. Soc.* **2018**, *140*, 6014−6026.
(46) Mastalerz, M.; Oppel, I. M. Rational Construction of an Extrinsic Porous Molecular Crystal with an Extraordinary High Specific Surface Area. *Angew. Chem. Int. Ed* **2012**, *51*, 5252−5255.
(47) Yang, Y.; Li, L.; Lin, R. B.; Ye, Y.; Yao, Z.; Yang, L.; Xiang, F.; Chen, S.; Zhang, Z.; Xiang, S.; Chen, B. Ethylene/Ethane Separation in a Stable Hydrogen-Bonded Organic Framework through a Gating Mechanism. *Nat. Chem.* **2021**, *13*, 933−939.
(48) Lü, J.; Perez-Krap, C.; Suyetin, M.; Alsmail, N. H.; Yan, Y.; Yang, S.; Lewis, W.; Bichoutskaia, E.; Tang, C. C.; Blake, A. J.; Cao, R.; Schröder, M. A Robust Binary Supramolecular Organic Framework (SOF) with High CO_2 Adsorption and Selectivity. *J. Am. Chem. Soc.* **2014**, *136*, 12828−12831.
(49) Holman, K. T.; Pivovar, A. M.; Swift, J. A.; Ward, M. D. Metric Engineering of Soft Molecular Host Frameworks. *Acc. Chem. Res.* **2001**, *34*, 107−118.
(50) Boer, S. A.; Morshedi, M.; Tarzia, A.; Doonan, C. J.; White, N. G. Molecular Tectonics: A Node-and-Linker Building Block Approach to a Family of Hydrogen-Bonded Frameworks. *Chem.—Eur. J.* **2019**, *25*, 10006−10012.
(51) Brekalo, I.; Deliz, D. E.; Barbour, L. J.; Ward, M. D.; Friščić, T.; Holman, K. T. Microporosity of a Guanidinium Organodisulfonate Hydrogen−Bonded Framework. *Angew. Chem. Int. Ed* **2020**, *59*, 1997−2002.
(52) Mu, Z.; Zhu, Y.; Li, B.; Dong, A.; Wang, B.; Feng, X. Covalent Organic Frameworks with Record Pore Apertures. *J. Am. Chem. Soc.* **2022**, *144*, 5145−5154.
(53) Hisaki, I.; Nakagawa, S.; Ikenaka, N.; Imamura, Y.; Katouda, M.; Tashiro, M.; Tsuchida, H.; Ogoshi, T.; Sato, H.; Tohnai, N.; Miyata, M. A Series of Layered Assemblies of Hydrogen-Bonded, Hexagonal Networks of C_3-Symmetric π-Conjugated Molecules: A Potential Motif of Porous Organic Materials. *J. Am. Chem. Soc.* **2016**, *138*, 6617−6628.
(54) Hisaki, I.; Ikenaka, N.; Gomez, E.; Cohen, B.; Tohnai, N.; Douhal, A. Hexaazatriphenylene-Based Hydrogen-Bonded Organic Framework with Permanent Porosity and Single-Crystallinity. *Chemistry* **2017**, *23*, 11611−11619.
(55) Suzuki, Y.; Gutiérrez, M.; Tanaka, S.; Gomez, E.; Tohnai, N.; Yasuda, N.; Matubayasi, N.; Douhal, A.; Hisaki, I. Construction of Isostructural Hydrogen-Bonded Organic Frameworks: Limitations and Possibilities of Pore Expansion. *Chem. Sci.* **2021**, *12*, 9607−9618.
(56) Ma, K.; Li, P.; Xin, J. H.; Chen, Y.; Chen, Z.; Goswami, S.; Liu, X.; Kato, S.; Chen, H.; Zhang, X.; Bai, J.; Wasson, M. C.; Maldonado, R. R.; Snurr, R. Q.; Farha, O. K. Ultrastable Mesoporous Hydrogen-Bonded Organic Framework-Based Fiber Composites toward Mustard Gas Detoxification. *Cell Rep. Phys. Sci.* **2020**, *1*, 100024.
(57) Schneemann, A.; Bon, V.; Schwedler, I.; Senkovska, I.; Kaskel, S.; Fischer, R. A. Flexible Metal-Organic Frameworks. *Chem. Soc. Rev.* **2014**, *43*, 6062−6096.
(58) Cui, P.; Svensson Grape, E.; Spackman, P. R.; Wu, Y.; Clowes, R.; Day, G. M.; Inge, A. K.; Little, M. A.; Cooper, A. I. An Expandable Hydrogen-Bonded Organic Framework Characterized by Three-Dimensional Electron Diffraction. *J. Am. Chem. Soc.* **2020**, *142*, 12743−12750.
(59) Adams, P. D.; Afonine, P. V.; Grosse-Kunstleve, R. W.; Read, R. J.; Richardson, J. S.; Richardson, D. C.; Terwilliger, T. C. Recent Developments in Phasing and Structure Refinement for Macromolecular Crystallography. *Curr. Opin. Struct* **2009**, *19*, 566−572.
(60) Pulido, A.; Chen, L.; Kaczorowski, T.; Holden, D.; Little, M. A.; Chong, S. Y.; Slater, B. J.; McMahon, D. P.; Bonillo, B.; Stackhouse, C. J.; Stephenson, A.; Kane, C. M.; Clowes, R.; Hasell, T.; Cooper, A. I.; Day, M. G. Functional Materials Discovery Using Energy-Structure-Function Maps. *Nature* **2017**, *543*, 657−664.

Recommended by ACS

Thermally Conductive Self-Healing Nanoporous Materials Based on Hydrogen-Bonded Organic Frameworks
Muhammad Akif Rahman, Ashutosh Giri, *et al.*
OCTOBER 19, 2022
NANO LETTERS
READ

Covalent Organic Frameworks with Record Pore Apertures
Zhenjie Mu, Xiao Feng, *et al.*
MARCH 08, 2022
JOURNAL OF THE AMERICAN CHEMICAL SOCIETY
READ

Supramolecular Organic Frameworks: Exploring Water-Soluble, Regular Nanopores for Biomedical Applications
Zhan-Ting Li, Dan-Wei Zhang, *et al.*
AUGUST 02, 2022
ACCOUNTS OF CHEMICAL RESEARCH
READ

Recovery of MOF-5 from Extreme High-Pressure Conditions Facilitated by a Modern Pressure Transmitting Medium
Samuel J. Baxter, Andreas Schneemann, *et al.*
JANUARY 07, 2022
CHEMISTRY OF MATERIALS
READ

Get More Suggestions >

https://doi.org/10.1021/accountsmr.2c00173
Acc. Mater. Res. XXXX, XXX, XXX−XXX